Direction of Tornado Motions and Its Relationship with the Large-scale Wind Field

Yuri Mita and Tsubasa Kohyama

Department of Information Sciences, Ochanomizu University, Tokyo, Japan

February 19, 2024

Corresponding author: Yuri Mita, Department of Information Sciences, Ochanomizu University, 2-1-1, Otsuka, Bunkyo-ku, Tokyo, 112-8610, Japan.

E-mail: mita.yuri@is.ocha.ac.jp

Abstract

According to Niino et al. (1997), more than half of tornadoes in Japan from 1961 to 1993 moved toward the northeast quadrant. However, since this data was based on visual observations, the reported directions of tornado motions were biased toward 8 directions out of 16. Therefore, using tornado records from the database of gusty winds of the Japan Meteorological Agency, our study collects directional data of tornado motions in an objective way, and investigates comprehensively the relationship between directions of tornado motions and the large-scale wind field. First, the direction of tornado movement is calculated from the latitudes and longitudes of the starting and ending points of the damage path. These calculations show that approximately 70% of tornadoes moved toward the northeast quadrant. The preference for the northeastward movement remains similar for the periods of 1961-1993 and 1994-2022, although the Japan Meteorological Agency changed several times their operation to collect tornado report data during the periods. This northeast preference is caused by the superposition of eastward and northward peaks. The eastward preference suggests that the cumulonimbus clouds are transported by the westerly wind at the middle troposphere to first order. In all seasons, a similar eastward preference is observed. In contrast, the distribution of the direction of movement of JJA and SON tornadoes exhibit a northward predominance, due to torna-

does associated with typhoons. The high correlations between the direction of tornado motions and the large-scale wind directions are also consistent with a notion that tornadoes are overall transported by winds along with cumulonimbus clouds. Nevertheless, predicting the direction of supercell movements using the method of Bunkers et al. (2000), the directions of tornado movements are found to deviate approximately 60° counterclockwise from the supercell movements on average. This result quantitatively suggests that many tornadoes in Japan are not necessarily supercell-type.

Keywords tornado; direction of movement; typhoon; supercell; circular statistics

1. Introduction

A tornado is a violent atmospheric vortex caused by an updraft in a cumulus or cumulonimbus cloud. Tornadoes are generated when atmospheric conditions are extremely unstable, and can cause extensive damage over a narrow band-like area in a short period of time. In addition to damage caused by tornadoes (Brooks and Doswell, 2002; Agee and Taylor, 2019) and the spatio-temporal distribution of the occurrences of tornadoes (Dessens and Snow, 1989; Taszarek and Gromadzki, 2017), the climatological aspects (Galway, 1977) and the effect of their synoptic scale phenomena on tornado occurrence have long been discussed (Tippett et al., 2016; Tochimoto, 2022). Despite these efforts, tornado occurrence has been difficult to predict. In the United States, where damage caused by tornadoes and waterspouts is common, previous studies have not only focused on the occurrence of tornadoes, but also on the directions and tracks of tornado movements (Notis and Stanford, 1976; Suckling and Ashley, 2006).

Prediction of the occurrence and track of tornadoes is essential to reduce damage on people and infrastructure. The frequency of tornado occurrence and the extent of damage are affected by weather conditions and geographical factors thus, different features are observed in each country. As tornadoes are relatively local phenomenons, they are rarely considered as a social issue in Japan, but they do cause damage. According to Kobayashi and Norose (2012), 1228 tornadoes occurred from 1961 to 2011 in Japan, and 42% of them caused human or property damage. The total number of deaths was 39 and the number of injuries was 2,022. Owing to the rugged terrain in Japan, few tornadoes have long damage paths, with an average damage path length and average width of 3.2 km and 98 m, respectively (Niino et al., 1997). Additionally, coastal areas, especially the Pacific coast, are prone to tornadoes (Hayashi et al., 1994). In areas with a large population, the possibility of severe damage from tornadoes is high, and if the weather becomes more unstable in the future, the concerns of people living along the coast may increase.

Many studies of developmental structure using numerical simulations have been conducted in Japan to investigate tornadoes. Recent studies extensively simulated a deadly tornado in Japan, which was spawned by the supercell in Tsukuba on May 6, 2012. In these numerical simulations, the vorticity source of mesocyclones was used to investigate the causes of tornado occurrence (Mashiko, 2016a,b; Yokota et al., 2018). Other previous studies have also used Doppler radar measurements and numerical simulations to investigate the vertical structure of cumulonimbus clouds and occurrence factors of tonadoes (e.g., Niino et al., 1993; Mashiko et al., 2009; Adachi and Mashiko, 2020).

However, the number of statistical studies on tornadoes is limited owing to the reliance on visual observation reports. As the most comprehensive statistical study on tornadoes in Japan, Niino et al. (1997) (hereafter NFW97) conducted a significant statistical analysis of tornadoes and waterspouts during 33 years from 1961 to 1993, and estimated the risk of tornado encounters in each prefecture. Other previous studies on tornado statistics in Japan include the following: general statistical studies that have proposed a scale for evaluating the strength of tornadoes based on damage (Fujita, 1971); statistical investigation of tornado characteristics by regions and weather conditions (Hayashi et al., 1994); and observational research reports (e.g., Suzuki et al., 2000; Kobayashi et al., 2008). Although previous studies have discussed the environmental fields suitable for tornado occurrence and their predictability before tornado occurrence (Sakurai and Kawamura, 2008; Shibata, 2006), little statistical research has been conducted on the subsequent movement of tornadoes, especially in the northwest Pacific.

This situation has motivated us to discuss the possibility of statistically predicting the direction of tornado movements after its occurrence. According to NFW97, more than 50% of tornadoes from 1961 to 1993 moved toward the northeast quadrant and approximately 22% moved northeastward (Fig. 1a). Nevertheless, these directions are not necessarily accurate as visual observation reports tend to be stated in eight major directions (i.e, $45^\circ \times n$ (integer) from the east), and NFW97 did not deeply investigate the reasons for the preference in the direction of tornado movement and the relationship with large-scale wind fields. Fig. 1

Therefore, in this study, we first calculate the direction of tornado movements, including occurring after NFW97, based on the starting and ending points of the damage path. Subsequently, we verify that the northeastward propensity remains the same in a more recent time period. Thereafter, we consider the characteristics of the distribution of the directions of tornado movement by categorizing tornado movements by seasons, regions of occurrence, and meteorological conditions at the time of occurrence. We then use circular statistics to determine the correlation between tornadoes and the mean wind. We also employ a method to predict the supercell movement to understand tornadoes that deviate from the mean wind. By doing so, we explore the cause of the propensity toward the northeast quadrant.

This article is organized as follows. The data used in this study are described in the following section. In the third section, after examining the statistics of the distribution of the directions of tornado movement, we show that the directions of tornado movement and tropospheric wind exhibit a statistically significant correlation. Furthermore, by predicting the directions of supercell movements to compare them with those of tornado movements, we examine the asymmetric drift relative to the mean wind. The summary, including future challenges, are presented in section 4.

2. Data and Methods

2.1 Directions of tornado movement

The tornado data used for statistical analyses are the database of gusty winds of the Japan Meteorological Agency (JMA). This database contains the records of 1,611 tornadoes between January 1961 and December 2022. From these samples, we extract 1,068 tornado cases, including the records of the time (on the second timescale) and location (latitude and longitude). Observational errors are not considered. Subsequently, we use the time and place of occurrence. The direction of tornado movement provided by JMA is not used because available data are limited for cases where the track has been determined or reported.

As shown in Fig. 1b, we calculat the direction of tornado movements using the starting and ending points of the damage path, without using visual observation reports or the wind direction at the surface. The direction of tornado movement θ_t is calculated using equation 1,

$$\theta_t \equiv \arctan \frac{R(\varphi_2 - \varphi_1)}{R \cos \overline{\varphi} (\lambda_2 - \lambda_1)} \tag{1}$$

where $\varphi_1(\varphi_2)$ and $\lambda_1(\lambda_2)$ represent the latitudes and longitudes of the starting (ending) points, respectively, and $\overline{\varphi} = (\varphi_1 + \varphi_2)/2$ denotes the mean latitude. R is the radius of the earth, namely, 6.4×10^6 m. If $\lambda_1 = \lambda_2$ ($\varphi_1 \neq \varphi_2$), θ_t is defined to be 90°. When presenting the statistics in 16 directions, all directions are divided into 16 pieces at intervals of 22.5°. For example, when θ_t is 0°, the movement is eastward.

The tornado case is extracted only if it moved for more than 1 second (approximately 40 m) in either latitudes or longitudes from the observed damage, and 650 cases are available during the statistical period (1961-2022) of this study. In the Appendix, we discuss whether it is appropriate to consider a tornado track as a straight line connecting the places of occurrence and extinction by ignoring the details of its complex movement.

2.2 Typhoon-related Tornadoes

Tornadoes that occur in conjunction with typhoons (hereafter referred to as typhoon-related tornadoes) are defined on the basis of the distance from the typhoon center. The tornado database of JMA has a list of candidates for related synoptic disturbances, and the number of estimated typhoon-related tornadoes is 144 out of the 650 tornadoes presented in section 2.1.

Nevertheless, as the precise definition is not provided, we have extracted the typhoon-related tornadoes as follows. We first obtain the location of the center of the typhoon from the Best Track Data of The Regional Specialized Meteorological Center (RSMC) at the closest time when a tornado was recorded by the JMA. If multiple typhoons occurred simultaneously, the one with the closest distance is used. Subsequently, a tornado is defined to be typhoon-related if its distance from the center of the typhoon is less than 1,500 km.

$$R\sqrt{(\cos\overline{\varphi}(\lambda_2-\lambda_1))^2+(\varphi_2-\varphi_1)^2} < 1,500 \text{ km} \tag{2}$$

The number of extracted typhoon-related tornadoes are 181, which is comparable with that of the JMA database.

2.3 Wind Directions

We use the reanalysis data of horizontal winds at specified pressure levels (300, 400, and 500 hPa, and at intervals of 50 hPa from 600 to 1000 hPa) provided by the European Medium-Range Weather Center (ECMWF) Reanalysis 5 (ERA5). The horizontal resolution is 0.25° in both zonal and meridional directions, and the temporal resolution is 1 h. At the time immediately preceding tornado occurrence, we use the mean of winds at four nearest neighbors of the point of occurrence for both zonal (u) and meridional (v) wind data. The angle of wind direction θ_w is calculated using equation 3,

$$\theta_w \equiv \arctan \frac{v}{u} \tag{3}$$

and if $u = 0$, θ_w is defined to be 90°. For example, the wind directions toward the east (i.e., westerly wind), north, and south are represented by θ_w values of 0°, 90°, and −90°, respectively.

2.4 Circular Statistics

Angular data poses a major problem when conducting statistical analysis. Notably, statistical analysis methods that target non-angular data cannot be used when analyzing angular data. This problem is caused by the fact that angles (or circumferences) have periodicity. For example, a mean value will have unnatural definitions if applied naively to angular data. The mean of 1° and 359° should not be $(1°+359°)/2 = 180°$, but should be 0°. The statistical analysis method for angular data is defined as circular statistics (e.g., Fisher et al., 1993; Mardia et al., 1999).

In this study, we calculate the correlations between two angular variables, tornado movement direction θ_t, and wind direction θ_w at the time of tornado occurrence using the circular correlation measure descrobed by Jammalamadaka et al. (2001). The circular correlation coefficient γ_c is defined as

$$\gamma_c \equiv \frac{\displaystyle\sum_{k=1}^{n} \sin(\theta_{tk} - \overline{\theta_t}) \sin(\theta_{wk} - \overline{\theta_w})}{\sqrt{\displaystyle\sum_{k=1}^{n} \sin^2(\theta_{tk} - \overline{\theta_t}) \sin^2(\theta_{wk} - \overline{\theta_w})}} \tag{4}$$

where the direction of tornado movement is θ_{tk}, that of the wind is θ_{wk}, and the sample size is denoted as n. Here, the mean values of θ_{tk} and θ_{wk} using circular statistics are represented by $\overline{\theta_t}$ and $\overline{\theta_w}$, respectively, and calculated as

$$\overline{\theta_i} \equiv \arctan \frac{\displaystyle\frac{1}{n}\sum_{k=1}^{n} \sin\theta_{ik}}{\displaystyle\frac{1}{n}\sum_{k=1}^{n} \cos\theta_{ik}} \quad (i = 1, 2) \tag{5}$$

Based on Jammalamadaka et al. (2001), the test statistic z_γ of two correlated variables is determined as

$$z_\gamma = \gamma_c \sqrt{\frac{n\alpha_{20}\alpha_{02}}{\alpha_{22}}}$$

where

$$\alpha_{ij} \equiv \frac{1}{n}\sum_{k=1}^{n} \sin^i(\theta_{tk} - \overline{\theta_t}) \sin^j(\theta_{wk} - \overline{\theta_w})$$

and the statistical confidence interval is calculated assuming that z_γ follows a standard normal distribution.

2.5 Estimation of supercell-type tornadoes

The causes of tornadoes in Japan range from large-scale disturbances, such as typhoons and cold fronts, to localized disturbances, and include both supercell and non-supercell types. A typical method for predicting the movement direction of supercells is proposed by Bunkers et al. (2000), and is referred to as the internal dynamics (ID) method. If most tornadoes in Japan are supercell-type, we can predict the movement of tornadoes along with that of supercells. To test whether most tornadoes are of the supercell-type, we calculate the movement vector of the supercell for each date and time of tornado occurrence, following the ID method.

We use the reanalysis data of horizontal wind at specified pressure levels (intervals of 100 hPa from 500 to 1000 hPa) provided by ERA5. The equations for the motion of right-moving (RM) and left-moving (LM) supercells are expressed as

$$\mathbf{V}_{\mathrm{RM}} = \mathbf{V}_{\mathrm{mean}} + D\left[\frac{\mathbf{V}_{\mathrm{shear}} \times \hat{\mathbf{k}}}{|\mathbf{V}_{\mathrm{shear}}|}\right] \tag{6}$$

$$\mathbf{V}_{\mathrm{LM}} = \mathbf{V}_{\mathrm{mean}} - D\left[\frac{\mathbf{V}_{\mathrm{shear}} \times \hat{\mathbf{k}}}{|\mathbf{V}_{\mathrm{shear}}|}\right] \tag{7}$$

Following Bunkers et al. (2000), $D = 7.5$ m/s is the relative speed of the supercell to the mean wind. $\mathbf{V}_{\mathrm{mean}}$ and $\mathbf{V}_{\mathrm{shear}}$ are the advective and propagation components, respectively. In this study, $\mathbf{V}_{\mathrm{mean}}$ is estimated as the mean wind vector from 500 to 1000 hPa (at intervals of every 100 hPa),

$\mathbf{V}_{\text{shear}}$ as the difference between the 500 and 1000 hPa winds, and $\hat{\mathbf{k}}$ denotes the unit vector along the vertical axis.

3. Results

First, using the JMA data and equation 1, we have compared our study with a previous study, and presented the geographical distribution of the directions of tornado movement in subsections 3.1 and 3.2. Subsequently, we further analyze the obtained data on the seasonality and their relationship with typhoons in subsections 3.3 and 3.4. Thereafter, in subsections 3.5 and 3.6, we indicate the relationship between tornado movement and the large-scale wind at the time of tornado occurrence. Additionally, in subsection 3.7, we discuss the relationship between the tornado and supercell movements. Last, in subsection 3.8, we have conducted similar analyses by focusing only on tornadoes that have caused more than a certain amount of damage.

3.1 Comparison with the previous study NFW97

First, to establish the statistical confidence of the directional predominance indicated in NFW97, we present statistics for the same period as in NFW97 and the subsequent period. During the same period, we have reproduced that the directions of tornado movement are concentrated in the northeast quadrant (Fig. 1c). Here, the northeast quadrant denotes the 90°-range counterclockwise from the east to the north. Among the 149 tornadoes that occurred between 1961 and 1993, 73% (109 cases) of them moved toward the northeast quadrant. While NFW97 consolidated the movement directions of 353 tornadoes over the same period, this study is limited to 149 cases. The reason for this discrepancy lies in the fact that, while NFW97 gathers tornado information from various reports by JMA and literature by local meteorological observatories, this study relies solely on the database of gusty winds currently provided by JMA.

The protrusions in 8 directions reported in NFW97 (Fig. 1a) became moderate, as shown in Fig. 1c. As previous indicated in NFW97, these protrusions are likely caused by the fact that people tend to state directions in these eight directions when presenting visual observation reports. In NFW97, northeast was the most frequent direction of tornadoes, at approximately 22%. Similarly, in our result, northeast is the most frequent, at 18%, followed by east, east-northeast, and north-northeast during the same period.

501 tornadoes that occurred between 1994 and 2022, which is after the time span of NFW97, are also analyzed similarly. Consequently, Fig. 1c shows that 64% (327 cases) of the tornadoes moved to the northeast quadrant. During this period, the east direction has the highest number of

tornado occurrences, at 17%, followed by north, east-northeast, and northeast. As the years progress, reports of smaller tornadoes with less damage increased, and this change is presumably the reason for the difference in the two shapes shown in Fig. 1c. The F1 tornadoes in the Fujita scale (hereafter referred to as the F scale), which roughly estimates wind speed based on the damage caused by gusts, such as tornadoes and downbursts, were 83% from 1961 to 1993 but 36% for the subsequent period. In both periods (i.e., 1961-1993 and 1994-2022), nearly half the tornadoes were concentrated within the 45° range from the east to the northeast. The qualitative results are the same for the two independent periods thus, the northeastward predominance is presumably not attributed to a sampling bias.

3.2 Geographical Distribution (1961-2022)

Tornadoes move to the northeast quadrant all over the Japanese mainland (Fig. 1d). Additionally, the occurrence of tornadoes are concentrated on the coast and in the Kanto Plain. Among all 650 tornadoes that occurred between 1961 and 2022, 66% (426 cases) of them moved to the northeast quadrant, comprising east (16%), east-northeast (13%), northeast (13%), north (13%), and north-northeast (10%) directions. The distribution of tornado occurrence is similar to that of previous statistical studies, with many tornadoes occurring along the coast, Kanto Plain, and plains of Miyazaki and Shizuoka. In Japan, with many mountainous areas, this distribution of tornadoes is mostly ascribed to the topography, but it also depends on the environment near the point of tornado occurrence (e.g., typhoons, fronts, and low pressure systems).

3.3 Seasonal Distribution

More than 60% of the tornadoes that occur in Japan move toward the northeast quadrant in all seasons. Figure 2a shows the number of tornadoes observed in June-July-August (JJA) and September-October-November (SON), when the number of tornado occurrences is particularly high. SON experiences the highest number of cases of 321, followed by JJA (178 cases), December-January-February (DJF, 78 cases), and March-April-May (MAM, 73 cases). In these cases, 60, 65, 82, and 74% of tornadoes in SON, JJA, DJF, and MAM, respectively, moved to the northeast quadrant. Fig. 2

In JJA and SON, the number of tornadoes exhibits peaks in both the east and north directions (Fig. 2a). In particular, in SON, almost the same number of tornadoes move toward the east and north (among the 321 tornadoes in SON, 53 and 47 tornadoes move to the north and east, respectively). This bimodal feature is particularly interesting because when considering all seasons, tornado movement exhibits moderate preference toward the northeast quadrant. As these two peaks are seasonal, in the next subsection, we discuss tornadoes associated with typhoons, which are common during this season.

In DJF and MAM, when tornado occurrences are relatively rare, tornadoes often occur on the side of Sea of Japan. 21 and 19% of tornadoes in DJF and MAM, respectively, moved to the east and more than half of them moved from east to northeast in both seasons.

The peaks to the north are observed only in JJA and SON, suggesting that tornado movement and its meteorological conditions are closely related, although the spatial and temporal scale of tornadoes is extremely small. The map in Fig. 2b shows the geographical distribution of tornado in JJA and SON. Tornadoes during these two seasons are frequently observed in the Pacific coast and plains, and show little difference in their geographical distribution.

3.4 Relationship with Typhoons

As specified in the previous subsection, 47 and 53 tornadoes moved eastward and northward, respectively, among the 321 cases in SON. Presumably, these two peaks are observed owing to different mechanisms, and the northward peak is observed only from July to October. Therefore, in this subsection, we investigate the relationship of tornadoes with typhoons because tornadoes occurring intensively in these seasons are occasionally related to typhoons.

Typhoons are one of the main weather conditions of tornadoes (Niino et al., 1997). According to Hayashi et al. (1994), the number of typhoons since the 1980s has not decreased compared with that in the previous years, but the annual number of tornadoes caused by typhoons has decreased. However, based on the data used in this study, we observed 31 cases in the first 20 years (1961-1980), 24 cases in the next 20 years (1981-2000), and 81 cases in the next 22 years (2001-2022) thus, this number is actually increasing. This increase is likely attributed to an increase in the number of reported cases since 2000 and to changes in operation of damage surveys by the JMA several times, and may not be a real upward trend in the number of cases.

We extract 64 and 114 cases of tornadoes occurring with typhoons in JJA and SON. The definition of typhoon-related tornadoes is described in section 2.2. Typhoon-related tornadoes move most frequently to the north (Fig. 3a), whereas typhoon-unrelated tornadoes to the east (Fig. 3b). These two peaks are consistent with the observational evidence suggesting that 65% of all tornadoes from 1961 to 2022 moved to the northeast quadrant (subsection 3.2).

More than 70% of typhoon-related tornadoes (73 and 76% for JJA and SON, respectively) are concentrated in the northern quadrant (northeast to the northwest), and few moved eastward. In contrast, approximately 70% (72 and 65% for JJA and SON, respectively) of typhoon-unrelated tornadoes moved to the northeast quadrant. Thus, the peak to the north is presumably caused by typhoon-related tornadoes. Fig. 3

The reason why tornadoes associated with typhoons move to the north is that most tornadoes occur in the northeast quadrant of a typhoon (e.g., Kobayashi et al., 2007; McCaul, 1991), which has a counterclockwise circulation, yielding southerly winds in the environmental fields. Based on the JMA data, more than 80% of typhoon-related tornadoes occurred in the northeast quadrant relative the typhoon, and nearly a half of these tornadoes particularly occurred in the 22.5°-range of the northeast direction. A similar directional bias in the incidence of tornado events, rather than their movement after their occurrence, is also reported for hurricanes (e.g., Novlan and Gray, 1974; Gentry, 1983).

3.5 Correlations with the large-scale wind field at each pressure level

The wind direction at the time of tornado occurrence is mainly westward, and is mostly toward the northeast quadrant, regardless of the altitude (Fig. 4a). As mentioned above, as eastward movements are the most common in all seasons, we hypothesize that to first order, the direction of tornado movement is determined by the movement of cumulonimbus clouds steered by the westerly winds in the middle troposphere. Therefore, in this subsection, we calculate the angular correlations between the directions of tornado movement and wind. Fig. 4

First, we focus on the 500 hPa level, which is present at an altitude of approximately 5.5 km in the middle troposphere. Figure 4b shows the scatter plot between the wind direction and direction of tornado movement. At the time of tornado occurrence, 75% of the winds blew toward the northeast quadrant. To investigate the relationship between wind and tornadoes moving toward the northeast quadrant, we hereafter only consider tornadoes whose wind direction and movement direction are within $-45° < \theta \leq 135°$ (524 cases at the 500 hPa level; the black box shown in Fig. 4b). The correlation coefficient between the directions of tornadoes movement and wind at the 500-hPa level is 0.58 (Fig. 4c), which is statistically significant at the 95% confidence level.

We similarly calculate the correlations at each pressure level from 300 to 1000 hPa (Fig. 4c). The 500-700 hPa layer exhibits the strongest correlation, and this correlation gradually decreases with decreasing altitude toward the surface of the Earth. This decrease occurres because as inferred from Fig. 4a, the northeastward predominance in wind direction becomes weaker with decreasing altitude. Both typhoon-related and typhoon-unrelated tornadoes have less strong correlations than in the total case, and the correlations are almost the same in both cases.

3.6 Directional drifts relative to tropospheric winds

Among tornadoes that occurred from 1961 to 2022, the directions of tornado movement and wind were most often the same, confirming the high correlation presented in subsection 3.5. Figure 5a shows the difference between the directions of tornado movement and wind at the 500 hPa level, $\theta_t - \theta_w$, i.e., the angle at which a tornado moves relative to the 500 hPa wind. In 292 out of the 650 cases, the directions of the winds and tornado movements are within 30° of each other. Fig. 5

If looked at closely, however, Fig. 5a shows a difference in the ratio between clockwise and counterclockwise drifts, and it is asymmetrical. In 62% (405 cases) of all cases, the direction of tornado movement is within 90° counterclockwise, relative to the wind direction. In contrast, the directions of tornado movement in only 24% (158 cases) of the cases are within 90° clockwise.

This asymmetry is also observed in typhoon-related tornadoes. In Fig. 5b, 144 tornadoes associated with typhoons are similarly illustrated. Although the number of tornadoes within 30° is small (59 cases), 128 tornadoes travel within 90° counterclockwise from the wind, accounting for

70% of the total. The number of clockwise tornado cases is 18, which is an overwhelmingly smaller number than the case shown in Fig. 5a.

3.7 Determination of supercell-type tornadoes and its relationship with tornado movements

To understand the mechanism of the drifts presented in subsection 3.6, we investigate the relationship between supercells and tornadoes in Japan, by calculating the direction of supercell movements. Supercells cause extremely severe storms, including tornadoes, and the supercells propagate to the left and right in response to the vertical wind shear of environmental winds. The ID method proposed by Bunkers et al. (2000), which uses hodograph techniques, is a standard procedure to predict supercell movements, including atypical supercells. A typical profile yields RM supercells, and most violent tornadoes are produced by supercells (e.g., Moller et al., 1994).

By hypothesizing that all tornadoes in Japan are of the supercell type, we follow the ID method to approximate the movement direction vector of the RM supercell that drives the tornado (see subsection 2.5). Although the conclusion by Bunkers et al. (2000) states that the usefulness of this method depends on the presence of sufficient vertical wind shear for the occurrence of the supercell process, we use this method to obtain a rough estimate. As the data of tornado speed are unavailable, we only compare the directions of the supercell (referred to as θ_s) and tornado movements (θ_t).

Following the definition of RM supercells, 94% of the supercells drifted clockwise relative to the environmental wind (500 hPa layer). For most of the RM supercells, the angle $\theta_s - \theta_w$ falls within the range of 0° to −60°, with the mean being −30°. This result is consistent with those of a previous study by Maddox (1976), which proposed a simpler way to predict the movement of tornadoes through proximity soundings (i.e., storms, not necessarily supercells). They empirically found that supercells deviated approximately 30° clockwise from the mean wind direction.

Based on these calculations, few tornadoes are found to be of the supercell-type. As shown in Fig. 5c, on average, the direction of tornado movement θ_t is approximately 35° counterclockwise away from θ_s. Only 181 tornadoes moved within 30° from θ_s, accounting for less than 30%.

Typhoon-related tornadoes are also not supercell-type, as expected, and drift counterclockwise more than all cases (Fig. 5d). The asymmetric drifts presented in subsection 3.6 occur as tornadoes tend to move more counter-clockwise (LM) relative to the mean wind, whereas supercells tend to move clockwise (RM).

Notably, many tornadoes move along with the supercell direction if supercells are assumed to be LM supercells relative to the mean wind (Fig.

5e). Therefore, we have made the following speculations regarding the influence of large-scale fields on the occurrence of tornadoes. In general, RM supercells are cyclonic, and LM supercells are anticyclonic. Cyclonic vortices develop in large-scale fields with the help of the Coriolis force thus, so the energy is easily amplified and manifests as supercells. In contrast, anticyclonic vortices are prohibited to develop strongly in large-scale fields. Hence, anticyclonic vortices may not manifest as supercells, but may result in tornadoes by the cascading of energy on smaller meteorological scales. Nevertheless, this speculation does not match the rotational direction of the tornadoes from observational reports, and is only consistent with energy. In the JMA database, the directions of rotation of only approximately 30% (193 cases) of all tornadoes are recorded, and 18 tornadoes, less than 10%, were reported to be anticyclonic (clockwise). Niino et al. (1997) also reported that 15% of all tornadoes were anticyclonic. As supercell-type tornadoes tend to be more violent than non-supercell-type tornadoes (Brooks and Doswell III, 2001), cases with a clockwise rotation may possibly be underestimated.

3.8 Tornadoes that caused more damage (F1 or higher)

From the perspective of disaster prevention, strong tornadoes that cause societal damage are especially important. When conducting the same analysis on tornadoes whose F-scale, a method to classify tornadoes based on the maximum level of damage, is F1 or higher, the results are consistent with those obtained in our study (Fig. 6). The number of these strong cases is 305, which is half the number of all the cases (650 cases).

The preference toward the northeast quadrant remains unchanged, but the distribution of movement directions is more evenly prominent to the east and the north (Fig. 6a). Compared with that of the results for all cases, the difference in prominence of tornado movement is because many of the strong cases are tornadoes associated with typhoons. In particular, 112 cases are associated with typhoons, and 193 are without typhoons for strong tornadoes. This is in contrast to the 181 cases with typhoons and 469 cases without typhoons for all the cases. We investigated the relationship between the direction of tornado movement and, the movement of 500 hPa winds and RM supercells, in the same way as subsection 3.6, 3.7, but the shape of the histogram does not change. Fig. 6

4. Summary

Approximately 70% of tornadoes that occurred in Japan from 1961 to 2022 moved to the northeast quadrant. We have confirmed the preference in the movement direction indicated in the previous study, namely, NFW97, by calculating the direction in a more objective manner using the starting and ending points of the damage path. This preference has not changed between the NFW97 (1961-1993) and subsequent periods (1994-2022), and the direction of tornado movement is predominantly from the east to the north throughout Japan. This predominance is observed throughout the seasons, but the distribution of tornadoes occurring in JJA and SON show sharp peaks in the north and east directions. By classifying tornadoes according to whether they occur in association with typhoons or not, the peak of the frequency to the north are largely explained by typhoons, while that to the east is caused by a mid-level flow in an environment without typhoon.

To predict the direction of tornado movements, we should pay attention to the troposphere as according to a first-order approximation tornadoes move in the same direction as the large-scale wind field. Using circular statistics, we have confirmed statistically significant correlations between the directions of tornado movement and wind throughout the entire tropospheric layer. However, more tornadoes drift counterclockwise than clockwise. Many tornadoes move more than 35° to the left relative to the mean wind. This direction is opposite to the movement of typical supercells, which tend to move to the right relative to the mean wind. Based on this result, many tornadoes that occur in Japan are suggested to not belong to be the supercell-type. Careful examination is required to understand the direction of drifts realtive to the wind fields.

Based on our results, as a simplest approach, disaster prevention measures could be taken by issuing a warning to the northeastward area immediately after the observation of a tornado. Furthermore, this study has demonstrated that the tornado movement is nearly similar to the movement of the parent storm or the environmental wind to first order. Therefore, utilizing the movement of storms observed by radar, specifically based on the nowcasting system provided by JMA or other weather service companies, could aid in determining the direction of tornado movement. Presently, predicting and detecting tornado occurrences remain challenging, with the hit rate of tornado cautionary information provided by JMA generally remaining around 5%. However, in the future, narrowing the range of warnings by incorporating the direction of tornado movement could not only reduce accidents but also enhance public disaster preparedness awareness.

Nevertheless, in this study, we have statistically investigated the predominance in the direction of tornado movement by ignoring details, such as the strength of the tornado and occurrence region. From the perspective of disaster prevention, the direction of tornado movement can be estimated by considering details of regional characteristics for tornadoes (e.g., facing the sea or large mountain range), and by using data with a finer spatial resolution.

Data Availability Statement

Tornado data analyzed in this study are available at https://www.data.jma.go.jp/stats/data/bosai/tornado/index.html, horizontal wind data analyzed in this study are available at https://cds.climate.copernicus.eu/cdsapp#!/dataset/reanalysis-era5-pressure-levels?tab=form, and typhoon track data analyzed in https://www.jma.go.jp/jma/jma-eng/jma-center/rsmc-hp-pub-eg/besttrack.html

Acknowledgements

The second author is supported by JSPS-Kakenhi 20K14554, 22H04487, 23H01241, and 23K13169. We would like to thank Editage (www.editage.jp) for English language editing.

References

Adachi, T., and W. Mashiko, 2020: High temporal-spatial resolution observation of tornadogenesis in a shallow supercell associated with Typhoon Hagibis (2019) using phased array weather radar. Geophys. Res. Lett., **47(19)**, e2020GL089635.

Agee, E., and L. Taylor, 2019: Historical analysis of us tornado fatalities (1808–2017): Population, science, and technology. Weather, climate, and society, **11(2)**, 355–368.

Brooks, H., and C. A. Doswell III, 2001: Some aspects of the international climatology of tornadoes by damage classification. Atmos. Res., **56(1-4)**, 191–201.

Brooks, H. E., and C. A. Doswell, 2002: Deaths in the 3 May 1999 Oklahoma City tornado from a historical perspective. Wea. Forecasting, **17(3)**, 354–361.

Bunkers, M. J., B. A. Klimowski, J. W. Zeitler, R. L. Thompson, and M. L. Weisman, 2000: Predicting supercell motion using a new hodograph technique. Wea. Forecasting, **15(1)**, 61–79.

Dessens, J., and J. T. Snow, 1989: Tornadoes in France. Wea. Forecasting, **4(2)**, 110–132.

Fisher, N. I., T. Lewis, and B. J. Embleton, 1993: Statistical Analysis Of Spherical Data. Cambridge Univ. Press.

Fujita, T. T., 1971: Proposed characterization of tornadoes and hurricanes by area and intensity. SMRP Research Paper 91, Univ. Chicago 42.

Galway, J. G., 1977: Some climatological aspects of tornado outbreaks. Mon. Wea. Rev., **105(4)**, 477–484.

Gentry, R. C., 1983: Genesis of tornadoes associated with hurricanes. Mon. Wea. Rev., **111(9)**, 1793–1805.

Hayashi, T., M. Yasushi, and I. Tohru, 1994: Statistics of tatsumaki in Japan (in Japanese). Annu. Disaster Prevention Res. Inst., Kyoto Univ. B, **37(B-1)**, 57–66.

Jammalamadaka, S. R., A. Sengupta, and A. Sengupta, 2001: Topics In Circular Statistics, Volume 5 of Series on Multivariate Analysis. World Scientific, 336.

Kobayashi, F., and K. Norose, 2012: Features of Human Damage Caused by Tornadoes in Japan. In Proc. Natl. Symp. Wind. Eng., Japan Association for Wind Engineering, 79–84.

Kobayashi, F., Y. Sugawara, M. Imai, and T. Maesaka, 2008: Wind speed of a waterspout occurred over Futtsu Coast on May 31, 2007. J. Wind. Eng., **33(2)**, 45–50.

Kobayashi, F., Y. Sugawara, and M. Matsui, 2007: Statistical characteristics of tornadoes in Japan during recent 10 years. In Summaries to Technical Papers of Annual Meeting 2007, Japan Association for Wind Engineering, Japan Association for Wind Engineering, 29–29.

Maddox, R. A., 1976: An evaluation of tornado proximity wind and stability data. Mon. Wea. Rev., **104(2)**, 133–142.

Mardia, K. V., P. E. Jupp, and K. Mardia, 1999: Directional Statistics, Volume 2 of Wiley Series in Probability and Statistics. John Wiley and Sons, Inc., 432.

Mashiko, W., 2016a: A numerical study of the 6 May 2012 Tsukuba City supercell tornado. Part I: Vorticity sources of low-level and midlevel mesocyclones. Mon. Wea. Rev., **144(3)**, 1069–1092.

Mashiko, W., 2016b: A numerical study of the 6 May 2012 Tsukuba City supercell tornado. Part II: Mechanisms of tornadogenesis. Mon. Wea. Rev., **144(9)**, 3077–3098.

Mashiko, W., H. Niino, and T. Kato, 2009: Numerical simulation of tornadogenesis in an outer-rainband minisupercell of Typhoon Shanshan on 17 September 2006. Mon. Wea. Rev., **137(12)**, 4238–4260.

McCaul, E. W., 1991: Buoyancy and shear characteristics of hurricane-tornado environments. Monthly Weather Review, **119(8)**, 1954–1978.

Moller, A. R., C. A. Doswell, M. P. Foster, and G. R. Woodall, 1994: The operational recognition of supercell thunderstorm environments and storm structures. Wea. Forecasting, **9(3)**, 327–347.

Niino, H., T. Fujitani, and N. Watanabe, 1997: A statistical study of tornadoes and waterspouts in Japan from 1961 to 1993. J. Climate, **10(7)**, 1730–1752.

Niino, H., O. Suzuki, H. Nirasawa, T. Fujitani, H. Ohno, I. Takayabu, N. Kinoshita, and Y. Ogura, 1993: Tornadoes in Chiba prefecture on 11 December 1990. Mon. Wea. Rev., **121(11)**, 3001–3018.

Notis, C., and J. L. Stanford, 1976: The synoptic and physical character of Oklahoma tornadoes. Mon. Wea. Rev., **104(4)**, 397–406.

Novlan, D. J., and W. M. Gray, 1974: Hurricane-spawned tornadoes. Mon. Wea. Rev., **102(7)**, 476–488.

Sakurai, K., and R. Kawamura, 2008: The Environment and Potential Predictability of Tornadoes occurred in japan. Tenki, **55(1)**, 7–22.

Shibata, N., 2006: Predictability of Tornado-Producing Supercell Associated with Typhoon -Environments and Characteristics of the Parent Storm of the Tornado in Hanyu city, Saitama Prefectureon 22 August 2001-. Tenki, **53(3)**, 197–205.

Suckling, P. W., and W. S. Ashley, 2006: Spatial and temporal characteristics of tornado path direction. The Professional Geographer, **58(1)**, 20–38.

Suzuki, O., H. Niino, H. Ohno, and H. Nirasawa, 2000: Tornado-producing mini supercells associated with Typhoon 9019. Mon. Wea. Rev., **128(6)**, 1868–1882.

Taszarek, M., and J. Gromadzki, 2017: Deadly tornadoes in Poland from 1820 to 2015. Mon. Wea. Rev., **145(4)**, 1221–1243.

Tippett, M. K., C. Lepore, and J. E. Cohen, 2016: More tornadoes in the most extreme US tornado outbreaks. Science, **354(6318)**, 1419–1423.

Tochimoto, E., 2022: Environmental controls on tornadoes and tornado outbreaks. Atmos.–Ocean, **60(3-4)**, 399–421.

Yokota, S., H. Niino, H. Seko, M. Kunii, and H. Yamauchi, 2018: Important factors for tornadogenesis as revealed by high-resolution ensemble forecasts of the Tsukuba supercell tornado of 6 May 2012 in Japan. Mon. Wea. Rev., **146(4)**, 1109–1132.

Appendix

In this study, the direction of tornado movement is defined as a straight line connecting the point of occurrence and extinction. To justify this definition based on the cases with detailed reports since 2000, we select two tornadoes in Japan that yielded long damage areas and a large social impact. The first case is a tornado caused by a front that occurred in the Saitama prefecture at 14:00 on September 2, 2013 Japan Standard Time (JST) (available at `https://www.data.jma.go.jp/obd/stats/data/bosai/tornado/2013090201/ref01.pdf`). This tornado was long lasting (30 minutes), strong (Fujita(F)-scale was F2), and the length of the affected area was long (19 km). Comparing the radar images provided by the JMA and the areas affected by tornadoes, the movement of the precipitating clouds and that of tornadoes match well. Although a slight meandering of the path was observed, the line drawn through the center of the path aligns with the east-northeast direction of the movement. The 500-hPa wind direction at this time is the northeast, and the tornado movement in the JMA's report is also the northeast.

Another typhoon-related tornado occurred in the Tochigi prefecture at 11:30 on August 10, 2014 JST (available at `https://www.data.jma.go.jp/obd/stats/data/bosai/tornado/2014081001/ref01.pdf`). This tornado was also strong (F1), lasted 20 minutes, had a damaged path length of 15 km, and occurred to the east-northeast of the typhoon. The center of the typhoon was approximately 550 km away from the tornado occurrence, but strong precipitating clouds existed in the area where the tornado occurred. Radar images show that it moved toward the north-northeast while slightly deviating from the southwesterly wind, which is consistent with the results of this study.

According to NFW97, the average length of the damage area of tornadoes in Japan is 3.2 km, so the majority of tornadoes are smaller and shorter than the two aforementioned examples. Therefore, even if the direction of movement is determined without considering the detailed meanderings of the movement track, it is useful at least as a first-order approximation. Nevertheless, the challenge is to analyze statistically while maintaining its accuracy. Although this study used the wind direction of vertically averaged wind over the troposphere as the environmental field, it could be more accurate to identify each cumulonimbus cloud to determine its direction of movement.

List of Figures

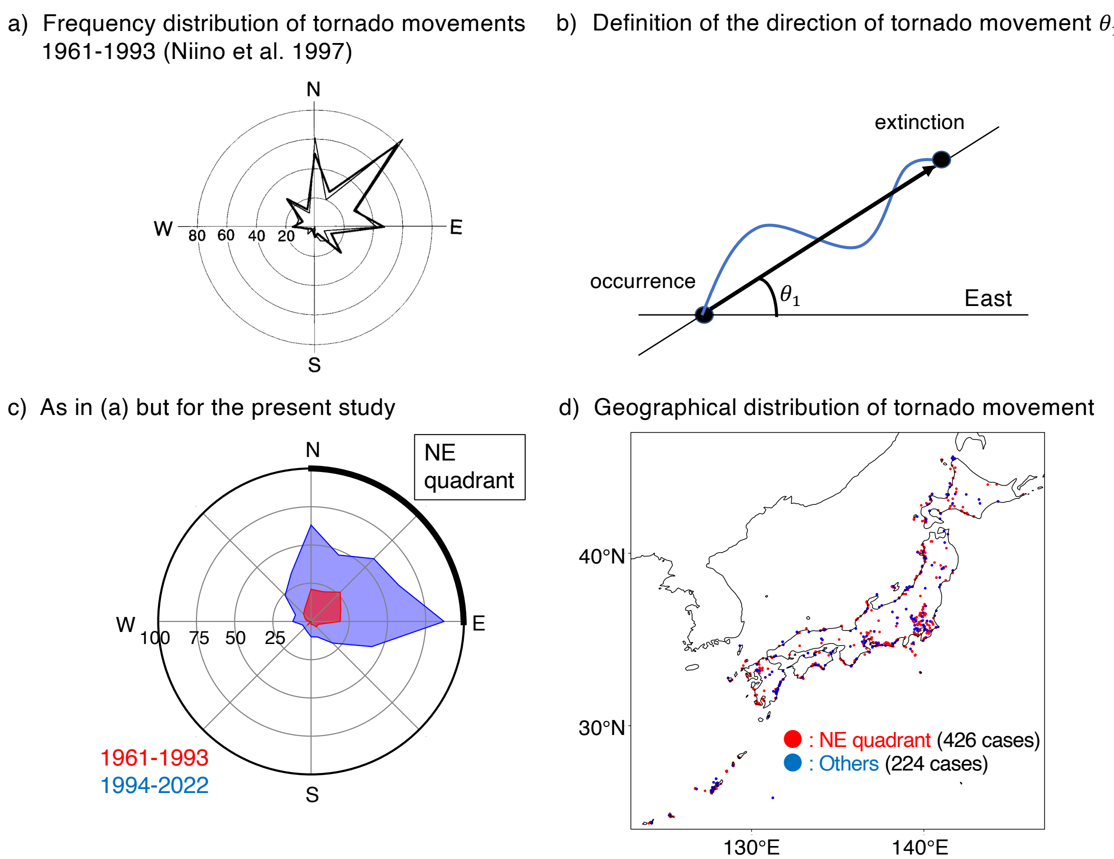

Fig. 1. a) Frequency distribution of the direction of tornado movements from 1961 through 1993 presented in Niino et al. (1997). b) Definition of the direction of tornado movement in this study. c) As in (a), but calculated using our definitions. d) Geographical distribution of tornado movement directions from 1961 through 2022.

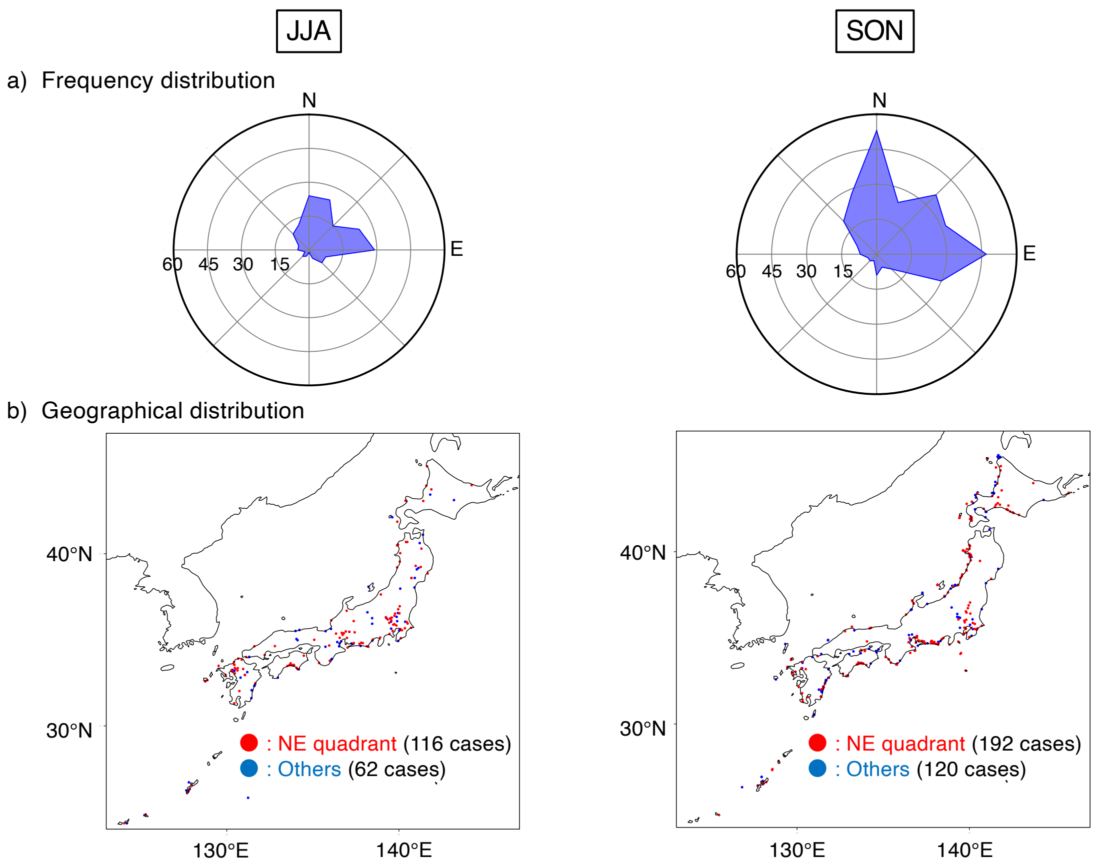

Fig. 2. a) Distribution of the direction of tornado movement that occurred in JJA (178 cases) and SON (321 cases). b) As in Fig. 1d, but for JJA (left) and SON (right).

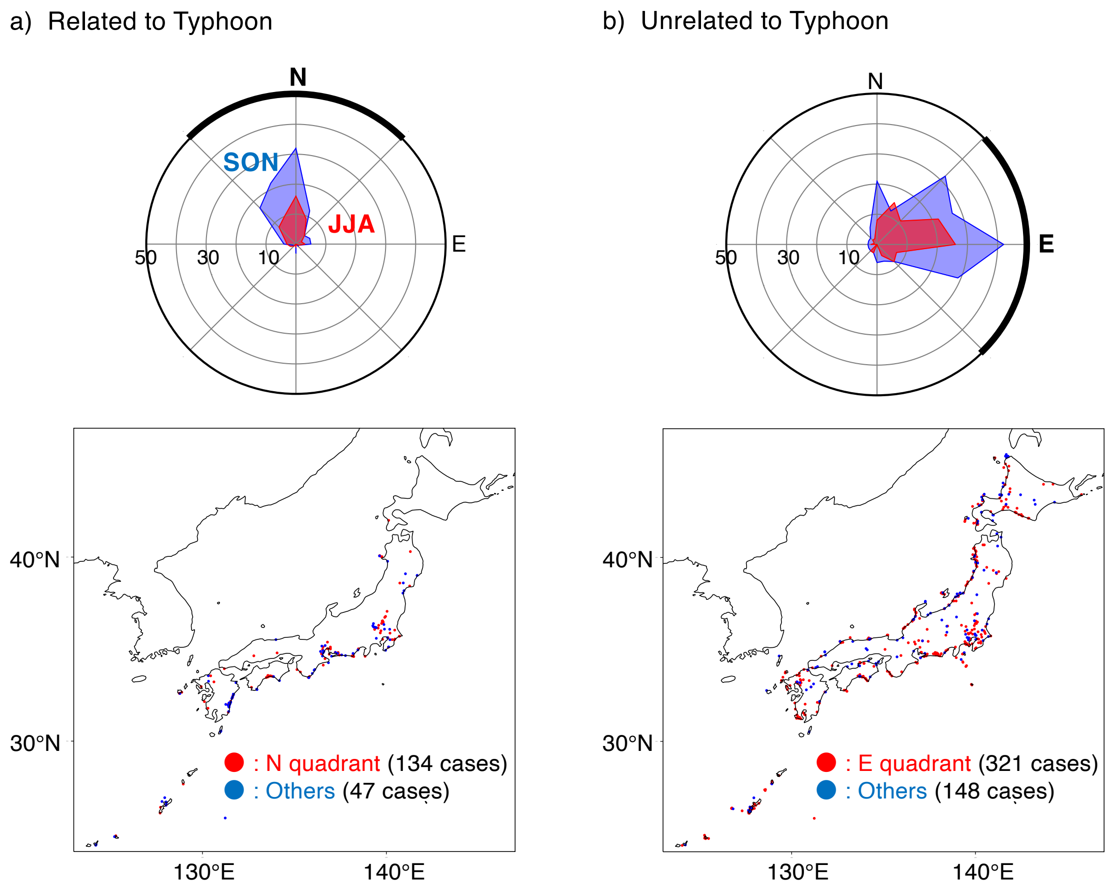

Fig. 3. Top: As in Fig. 2a, but for (a) typhoon-related and (b) typhoon-unrelated tornadoes. Bottom: As in Fig. 1d, but for (a) typhoon-related and (b) typhoon-unrelated tornadoes. Red markers denote the north and (b) the east quadrant.

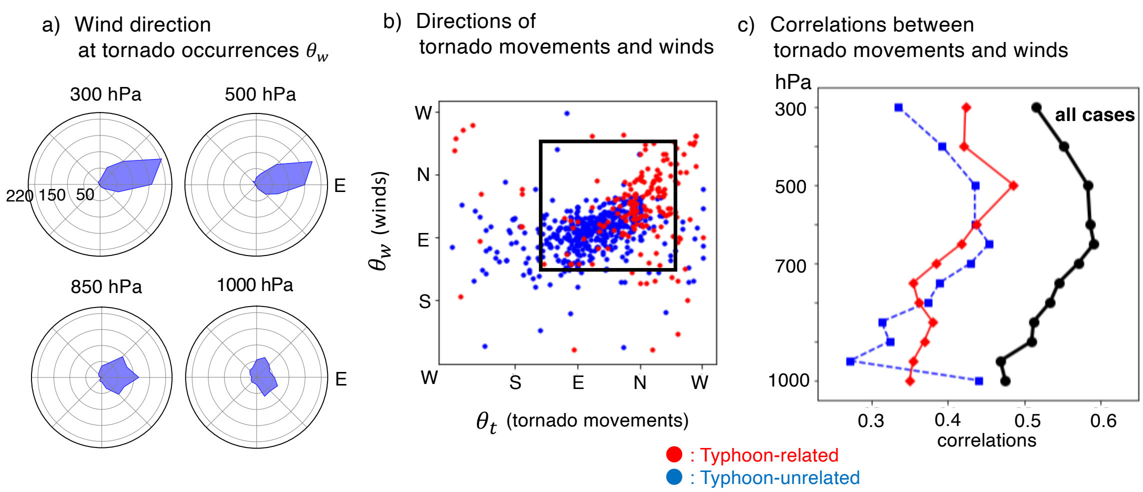

Fig. 4. a) Wind direction θ_2 at the time of tornado occurrence at 300, 500, 850 and 1000 hPa (650 cases each). b) Scatter plot of tornado movement direction θ_1 and wind direction θ_2. Typhoon-related (red) and typhoon-unrelated (blue) tornadoes are shown. c) Circular correlation coefficient between tornado movements and winds at each pressure level. Only data in the black box shown in (b) are used.

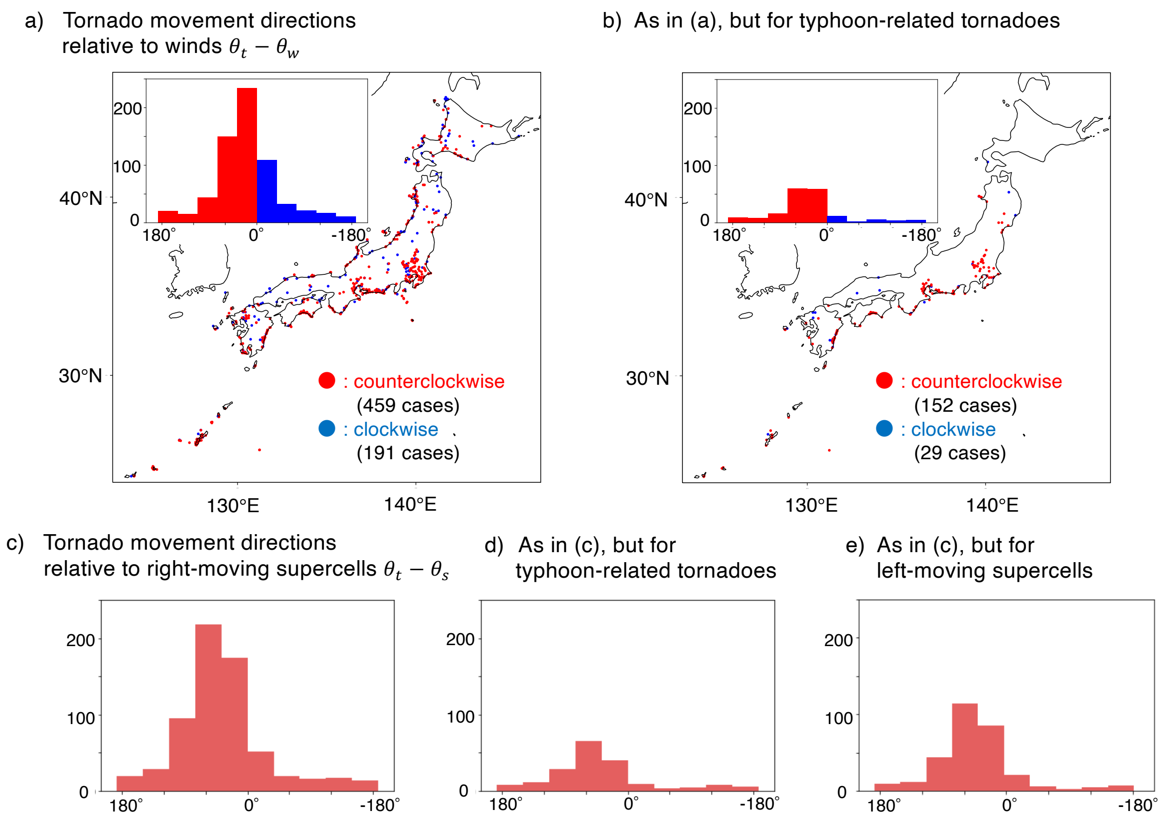

Fig. 5. a) Geographical distribution and the histogram of tornado movements relative to winds ($\theta_t - \theta_w$). A positive value (red) denotes the angle of the tornado movements counterclockwise relative to wind at the 500 hPa level, and a negative value (blue) denotes the angle clockwise relative to wind. b) As in Fig. 5a, but for typhoon-related tornadoes. c) Histogram of tornado movements relative to right-moving supercells ($\theta_t - \theta_s$). d) As in Fig. 5c, but for typhoon-related tornadoes. e) As in Fig. 5c, but for left-moving supercell movements

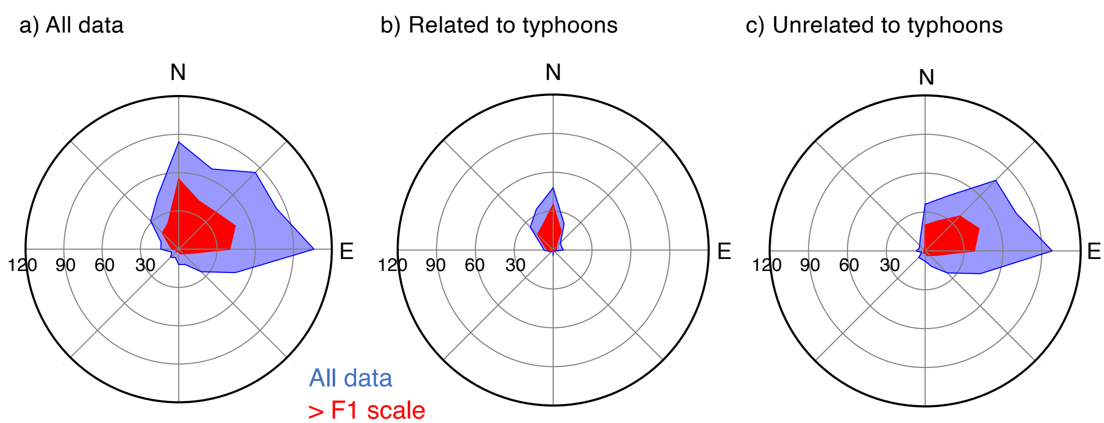

Fig. 6. a) Distribution of the direction of tornado movement for all tornadoes (blue) and those of F1 scale or higher (red) from 1961 through 2022. b) As in (a), but for typhoon-related tornadoes. c) As in (a), but for typhoon-unrelated tornadoes.